Hindawi
Advances in Materials Science and Engineering
Volume 2017, Article ID 7560468, 8 pages
https://doi.org/10.1155/2017/7560468

*Research Article*

# Optimizing Cutting Conditions and Prediction of Surface Roughness in Face Milling of AZ61 Using Regression Analysis and Artificial Neural Network

**Nabeel H. Alharthi,[1] Sedat Bingol,[2] Adel T. Abbas,[1] Adham E. Ragab,[3] Ehab A. El-Danaf,[1] and Hamad F. Alharbi[1]**

[1]*Department of Mechanical Engineering, College of Engineering, King Saud University, P.O. Box 800, Riyadh 11421, Saudi Arabia*
[2]*Department of Mechanical Engineering, Dicle University, 21280 Diyarbakir, Turkey*
[3]*Department of Industrial Engineering, College of Engineering, King Saud University, P.O. Box 800, Riyadh 11421, Saudi Arabia*

Correspondence should be addressed to Adel T. Abbas; atabbas1954@yahoo.com

Received 13 April 2017; Accepted 9 May 2017; Published 30 May 2017

Academic Editor: Belal F. Yousif



In this paper artificial neural network (ANN) and regression analysis were used for the prediction of surface roughness. Five models of neural network were developed and the model that showed best fit with experimental results was with 6 neurons in the hidden layer. Regression analysis was also used to build a mathematical model representing the surface roughness as a function of the process parameters. The coefficient of determination was found to be 94.93% and 93.63%, for the best neural network model and regression analysis, respectively, from the comparison of the models with thirteen validation experimental tests. Optical microscopy was conducted on two machined surfaces with two different values of feed rates while maintaining the spindle speed and depth of cut at the same values. Examining the surface topology and surface roughness profile for the two surfaces revealed that higher feed rate results in relatively thick roughness markings that are distantly spaced, whereas low values of feed rate result in thin surface roughness markings that are closely spaced giving better surface finish.

## 1. Introduction

Surface roughness is often taken as an important indicator of the quality of machined parts. The roughness influences the performance greatly in terms of mechanical parts as well as production cost. It is worth mentioning that surface roughness also influenced the mechanical properties such as corrosion resistance, creep life, and fatigue behavior. Extensive previous work [1–4] has been done on investigating the effect of the following parameters: cutting depth, feed rate, cutting speed, tool nose radius, lubrication condition, and cutting tool material, on the following response variables: tool wear, surface roughness, cutting forces, production time, and cost. These studies were conducted using different routes; analysis of variance, neural networking coupled with genetic algorithm, and neural networking coupled with electromagnetism optimization [5–10].

Magnesium, with a density of 1.8 g/cm$^3$, is considered to be the lightest structural metal. It is also one of the easiest metals to machine. Magnesium is often chosen because of its light weight. Its excellent machinability is a valuable advantage when a large amount of machining must be done. Less power is required for removing a given volume of magnesium by machining than for any other commonly machined metal. Heavy cuts can be taken at high speeds and feeds which can reduce machining time. Thus fewer machines, less capital investment, and less floor space and overhead costs are associated with machining magnesium and its alloys [5].

Chen et al. [6] applied the Taguchi methodology to investigate the effect of lubrication on turning TC11, feed and cutting depth, and velocity. The process response variables studied are cutting forces, surface roughness (Ra), and temperature on cutting zones. The results showed that for

orthogonal cutting the cutting depth is major parameter distressing cutting force and temperature, while the feed rate has major influence on the roughness. It was also reported that the cutting temperature, force, and surface roughness of diamond layered inserted tools were higher than uncoated, mainly with minimum quantity lubrication technology.

Azam et al. [7] investigated surface roughness (Ra) for turning high strength low-alloy steel (AISI 4340) using multilayer coated carbide tools. Response surface methodology (RSM) was utilized to improve the correlation between Ra and machining constraints (i.e., depth, speed, and feed). It was observed that the feed rate is the main constraint that affects surface roughness. The efficacy of the proposed model is confirmed through validation data with average estimate error of 3.38%.

Manivel and Gandhinathan [8] employed the Taguchi method to optimize the machining parameters (cutting speed, feed rate, depth of cut, and nose radius) in turning under dry condition using carbide inserts CVD coated with AL2O3/MT TICN. The analysis of variance (ANOVA) along with the signal to noise ratio were used to optimize the cutting parameters to minimize surface roughness and tool wear. It was reported that cutting speed is the most dominant factor affecting the response variables.

Raja et al. [9] implemented the Taguchi technique to analyze the results of turning AISI 316 and AISI 410 stainless steels. The process variables examined were feed rate, cutting speed, and depth of cut. Linear feed rate followed by quadratic feed rate were the most significant factors affecting surface roughness. Optimum cutting conditions for minimum surface roughness were identified for different cutting tool materials. The TiAlN composition coated insets gave the best performance.

Zhang et al. [10] investigated the finish turning of AISI 52100 bearing steel with low carbide born nitride (CBN) tools through an optimization process that applies Mixed Integer Evolutionary Algorithm (MIEA). Process parameters including tool geometry, cutting forces, and temperature were considered to minimize surface roughness and tool wear under practical constraints. The optimal design outcomes were validated against experimental and analytical work. The work showed that the proposed optimization technique had excellent search capability and computational efficiency for this mixed integer, constrained, highly nonlinear, nonexplicit, and not analytically differential optimization problem.

Jafarian et al. [11] predicted tool wear, cutting forces, and surface roughness using three artificial neural networks (ANN). An innovative process for training the ANNs using evolutionary algorithms rather than conventional systems that uses back-propagation was proposed. The optimization was carried to minimize surface roughness and cutting forces and maximize tool life in turning process. Genetic algorithm (GA) and particle swarm optimization (PSO) were employed to improve each output while keeping the rest of the outputs in the appropriate range. The acquired outcomes revealed that trained neural networks with genetic GA as an optimization objective functions present a potent tool to scrutinize the effect of each constraint on the output model with high accuracy level.

Mokhtari Homami et al. [12] employed a full factorial design complemented with artificial neural network (ANN) and subsequently optimization by genetic algorithm (GA) to study the main effects and interactions that minimize surface roughness and flank wear. It was reported that feed rate, nose radius, and approach angle had a significant effect on the flank wear and the surface roughness, but the cutting velocity had the most significant effect on the flank wear alone.

Jafarian et al. [13] applied neural networking and modified Nondominated Sorting Genetic Algorithm to optimize tool life and surface roughness in turning of Inconel 718 Super alloy. The work provided a strategy to give an efficient approach for tool life estimation in machining processes. It was reported that increasing the cutting speed and decreasing depth of cut and feed rate resulted in a better surface quality. Multiobjective optimization was implemented and the optimal conditions for maximizing tool life and minimizing surface roughness were identified.

Vaxevanidis et al. [14] investigated the machining of Ti-6Al-4V alloy, where spindle speed, feed rate, and depth of cut were taken as the process variables and the response variables were the main cutting force (Fz) and the average surface roughness (Ra). They reported that the application of this alloy is limited by tool wear and chattering. The results of 27 runs were analyzed using analysis of variance and showed strong interactions between process parameters. A feed forward back-propagation neural network was, also, developed to simulate the data. It was indicated that this approach can be utilized to predict and optimize Fz and Ra.

Senthil Babu and Vinayagam [15] have reviewed different methodologies for calculating surface roughness from machining constraints like depth, feed rate, and cutting speed. It has been reported (REF) that the electromagnetism (EM) algorithm coupled with back-propagation neural network is competent and specific system in attaining the lower surface roughness. However, a feed forward neural network model using Adaptive Particle Swarm Optimization (APSO) algorithm which has proven to be a very efficient process was proposed.

The objective of this paper is to compare the predicting capability of artificial neural network and regression analysis for surface roughness generated by different cutting conditions of spindle speed (rpm), feed rate (mm/min), and depth of cut (mm). In this paper, analysis of experimental data from Face Milling of AZ61 alloy will be conducted using five different ANN models and the results will be compared to the experimental results to select the model with the highest accuracy. The results from the best ANN model will then be compared to the results from a regression mathematical model.

## 2. Material and Methods

Chemical composition of Magnesium Alloy AZ 61, used in this study, is shown in Table 1.

Table 1: Chemical composition of magnesium AZ 61 alloy.

| Element | % by mass |
|---|---|
| Aluminum | 5.9 |
| Zinc | 0.9 |
| Copper | <0.03 |
| Silicon | <0.01 |
| Iron | <0.01 |
| Nickel | <0.005 |
| Magnesium | Balance |

Figure 1: Test rig for machining workpieces.

The machining of specimens was carried out on Emco-Mill Concept 45 CNC vertical milling machine. The machine was equipped with Sinumeric 840-D. The specimen surface area and height are 40 × 100 mm and 60 mm. The diameter of the cutter is 63 mm with 5 edges. To remove the high metal and quality surface finish, cutting tool with carbide inserts model face mill holder and Sandvik carbide coated inserts were used (i.e., Sandvik R245-063Q22-12M and Sandvik R245-12 T3M-PM4240). The cutter is of 5 edges with 63 mm diameter. The milling cutter was developed for heavy metal removal and mirror finishing. Furthermore, it is also fabricated with improved corners to reduce burr formation and dissipating of the component. The developed cutter is appropriate for face milling applications in diverse materials (i.e., stainless steel, steel, cast iron, aluminum, and titanium alloys) Figure 1 displays the test rig for machining workpieces. The test design was executed through 64 runs through a $4^3$ full factorial design. The runs were divided into 16 classes and each four classes were subjected to one common spindle speed (500, 1000, 1500, and 2000 rpm). All the classes were machined by four cutting depth levels (0.50, 1.0, 1.5, and 2.0 mm) and each depth was treated by feed rate having four levels (50, 100, 150, and 200 mm/min). Figure 2 demonstrated the model TESA Rugosurf 90-G, which is used to measure the surface roughness and ultimately surface topography. The list of samples and their surface roughness measurements are detailed in Table 4.

*2.1. Development of the ANN Model.* Artificial Neural Network (ANN) is a calculation method which is inspired from the behavior of human brain and neural system. ANN can recognize the complex relation between input and output data and then estimate the new results on the basis of

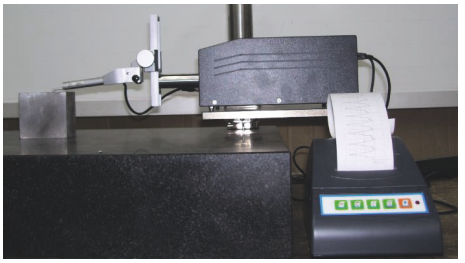

Figure 2: Test rig for measuring surface roughness Ra ($\mu$m).

experiences [16]. ANN is accepted for solution of the complex engineering systems efficiently. In this study, the usability of the ANN was examined to predict the surface Ra ($\mu$m) by the developed ANN models. The three parameters which are spindle speed (rpm), depth of cut (mm), and table feed (mm/min) were taken as input parameters to develop ANN models. The structure of the ANN used in this study with three inputs and one output is shown in the Figure 3. The used data for the developed ANN model is obtained from the performed experiments of this study. Different learning rules and structures can be used for an ANN. The common used ANN models are feed forward, multilayer perceptions trained by back-propagation based on gradient descent method. This algorithm can solve a continuous function approximately and shortly. The various ANN structures are established with the proper combinations of the input data to find the best model. In this study, 80% (51 experimental runs) of the total data was used to train the network while the rest of data, 20% (13 experimental runs), was used to test and validate the network. The validation test data was not used in the stage of training of the network, and this is a good indicator to test the accuracy of the developed ANN models. In addition, the best ANN model was developed among all tried models by changing the number of neurons on the hidden layer and using different transfer functions to estimate surface Ra ($\mu$m) successfully. The different variations of the neural structures have been employed to obtain convergence. Back-propagation algorithms and the feed forward neural networks composed multilayer detection have been conducted in this study.

*2.2. Development of Regression Model.* Multivariable regression analysis was used to build a mathematical model relating the process outcome (surface roughness Ra) with the three studied input parameters (spindle speed, depth of cut, and feed rate). The same 51 experiments used for training the ANN were used for the regression analysis. The remaining 13 experimental runs were used in testing both the regression and ANN models.

Regression was conducted using Minitab 17 software with stepwise technique to eliminate the insignificant terms from the model. The model was fitted in the form given by [2]

$$R_a = \beta_o + \sum_{i=1}^{k} \beta_i X_i + \sum_{i=1}^{k} \beta_{ii} X_i^2 + \sum \sum_{i<j} \beta_{ij} X_i X_j + \sum \sum_{i<j<k} \beta_{ijk} X_i X_j X_k + \sum \sum_{i \neq j} \beta_{iij} X_i^2 X_j + \epsilon_i, \quad (1)$$

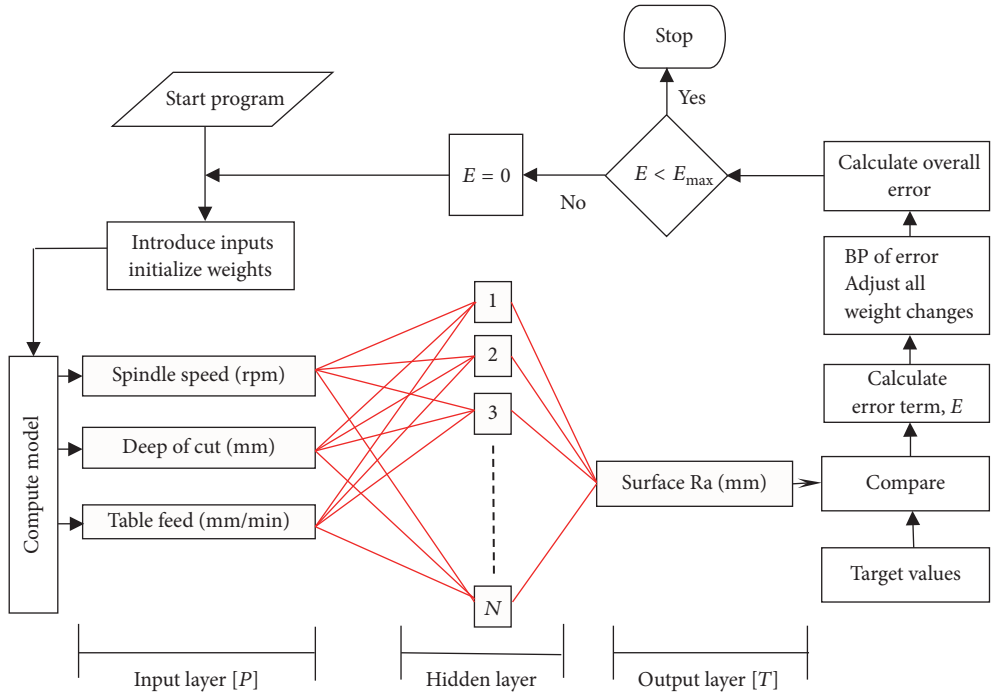


$N$: Number of neuron in hidden layer

Figure 3: Neural network structures to predict of the surface Ra ($\mu$m).

Table 2: Comparison of the developed different ANN structures for surface Ra ($\mu$m).

| ANN model | Algorithm | Function | Neuron number | $R$ | $R^2$ | MAE | MSE |
|---|---|---|---|---|---|---|---|
| Model 1 | Momentum | TanhAxon | 4 | 0.9319 | 0.8684 | 0.023 | 0.0008 |
| Model 2 | Momentum | Sigmoid Axon | 6 | 0.9074 | 0.8234 | 0.022 | 0.0006 |
| Model 3 | Levenberg | Sigmoid Axon | 10 | 0.8695 | 0.7560 | 0.034 | 0.0017 |
| Model 4 | Levenberg | TanhAxon | 6 | 0.9743 | 0.9493 | 0.015 | 0.0002 |
| Model 5 | Levenberg | TanhAxon | 12 | 0.9701 | 0.9411 | 0.015 | 0.0003 |

where $\beta_o$ is the constant term, $\beta_i$ represents the linear effects, $\beta_{ii}$ represents the pure quadratic effects, $\beta_{ij}$ represents the second level interaction effects, $\beta_{ijk}$ represents the third level interaction effects, $\beta_{iij}$ represents the effect of interaction between linear and quadratic terms, and $\epsilon_i$ represents the error in predicting experimental surface roughness.

Material removal rate (MRR) was calculated using (2) for each run. Desirability function approach was used to maximize MRR maintaining Ra below 0.4 $\mu$m as a maximum limit for the surface roughness value.

$$\text{MRR} = \text{DOC} * \text{Fr} * w, \tag{2}$$

where MRR is volume removed per unit time (mm$^3$/min.), DOC is depth of cut (mm), Fr is the feed rate (mm/min.), and $w$ is the width of cut (mm).

## 3. Results and Discussions

The developed neural network models and structures to estimate surface Ra ($\mu$m) are given in Table 2. Determination coefficient ($R^2$), mean square error (MSE), and mean absolute error (MAE), from the comparison with the 13 validation experimental tests are used for the statistical verification to evaluate the results of the developed ANN models. From Table 2, it can be seen that model 4 among the developed models in this study is the best model in terms of higher $R^2$ and lower MSE and MAE. The developed ANN models were also trained with the different neuron numbers to find ideal number in the hidden layer. The network optimization was started with four neurons in the hidden layer. Then, the number of neurons was increased from 4 to 12 to achieve the highest ($R^2$). As a result, the optimal number of neurons was decided as 6 with Levenberg algorithm and TanhAxon function (Table 2).

The regression fitted mathematical model is given by (3). Determination coefficient ($R^2$), mean square error (MSE), and mean absolute error (MAE) were calculated to be 0.847, 0.0005, and 0.017, respectively, for the 51 experiment runs used in the regression analysis.

$$\begin{aligned}\text{Ra} = {} & 0.2733 - 0.000212\text{SS} - 0.0645\text{DOC} \\ & + 0.001059\text{Fr} + 0.00000006\text{SS} * \text{SS} \\ & + 0.00004730\text{SS} * \text{DOC} - 0.00000026\text{SS} * \text{Fr}.\end{aligned} \tag{3}$$

Table 3: Comparison between regression model and ANN predictions.

| Machining parameters | | | Measured Ra | Regression model | | ANN | |
|---|---|---|---|---|---|---|---|
| SS | DOC | Fr | | Predicted Ra | Residual | Predicted Ra | Residual |
| 500 | 0.5 | 150 | 0.332 | 0.301 | 0.031 | 0.316 | 0.016 |
| 500 | 1 | 200 | 0.37 | 0.327 | 0.043 | 0.356 | 0.014 |
| 500 | 2 | 50 | 0.164 | 0.147 | 0.017 | 0.149 | 0.015 |
| 1000 | 0.5 | 100 | 0.184 | 0.193 | −0.009 | 0.158 | 0.026 |
| 1000 | 1 | 150 | 0.207 | 0.224 | −0.017 | 0.208 | −0.001 |
| 1000 | 1.5 | 200 | 0.258 | 0.255 | 0.003 | 0.272 | −0.014 |
| 1500 | 0.5 | 50 | 0.115 | 0.127 | −0.012 | 0.142 | −0.027 |
| 1500 | 1 | 100 | 0.181 | 0.164 | 0.017 | 0.162 | 0.019 |
| 1500 | 1.5 | 150 | 0.217 | 0.200 | 0.017 | 0.199 | 0.018 |
| 1500 | 2 | 200 | 0.235 | 0.237 | −0.002 | 0.218 | 0.017 |
| 2000 | 1 | 50 | 0.153 | 0.146 | 0.007 | 0.144 | 0.009 |
| 2000 | 1.5 | 100 | 0.155 | 0.188 | −0.033 | 0.169 | −0.014 |
| 2000 | 2 | 150 | 0.255 | 0.230 | 0.025 | 0.266 | −0.011 |

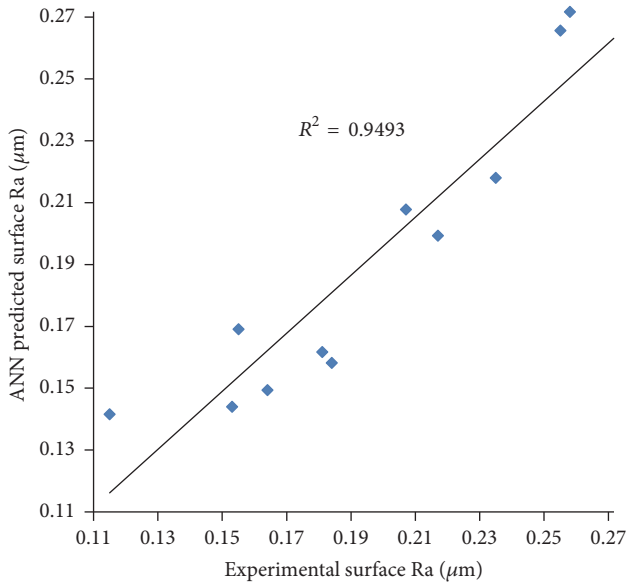


Figure 4: Experimental and ANN predicted results in the test period.

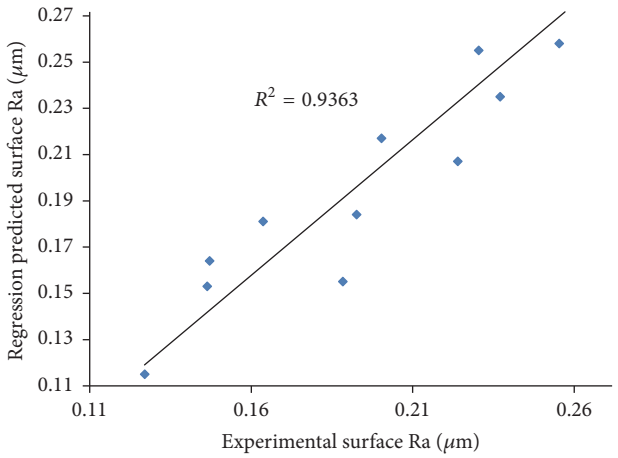


Figure 5: Experimental and regression predicted results.

Predictability of both regression and ANN models was compared using the 13 experimental validation cases that were not included in the modeling phase. Table 3 illustrates the results of this comparison. The ANN predictions are achieved using model 4 which exhibited the highest $R^2$ value. Experimental versus predicted results obtained from both ANN and regression are shown in Figures 4 and 5, respectively. It is clearly seen that there is a good agreement between the experimental results and the predicted results by both models.

Desirability function approach was used to estimate the values of studied process parameters that maximize the MRR keeping the Ra at levels not exceeding a practical value of 0.4 $\mu$m. The optimization plot, illustrated in Figure 6, shows that an optimum MRR of 13680 mm$^3$/min with Ra = 0.283 $\mu$m is obtained at spindle speed 500 rpm, depth of cut 2 mm, and feed rate 200 mm/min.

Surface roughness in AZ61 alloy was found to increase with increasing feed rate and depth of cut which both result in bigger cut areas that are consequently associated with higher cutting forces and higher friction which lead to poor surface finish. It was noticed from the surface roughness profile that high feed rates were associated with larger roughness markings horizontal spacing. Also, the vertical spacing between peaks and troughs of the surface irregularities was larger. Thus, higher feed rates led to higher surface roughness. Figure 7 represents an optical microscopy while Figure 8 represents the profile of surface roughness graph by surface roughness tester for the machined surface under spindle speed of 500 rpm, depth of cut of 0.5 mm, and table feed rate of 150 mm/min. Figure 9 represents an optical microscopy while Figure 10 represents the surface roughness profile by surface roughness tester for the following cutting conditions: spindle speed of 500 rpm, depth of cut of 0.5 mm, and table feed rate of 50 mm/min. The effect of feed rate is obvious, in a sense that low feed rate produced relatively thin surface roughness markings that are closely spaced, whereas high feed rate produced relatively thick roughness markings that are distantly spaced.

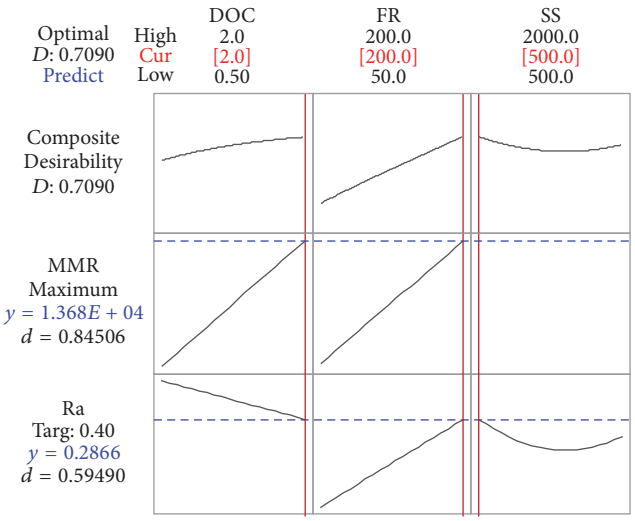


Figure 6: Optimization plot for Ra and MRR.

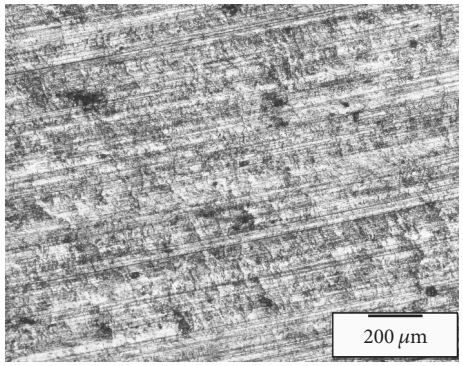


Figure 7: Optical microscopy for machined surface with speed 500 rpm, depth of cut 0.5 mm, and feed rate 150 mm/min.

## 4. Conclusions

In this study, an ANN model and regression analysis were developed to predict the surface Ra ($\mu$m) for different spindle speed (rpm), depth of cut (mm), and table feed (mm/min), in face milling of AZ61 magnesium alloy. Both models were compared with validation experimental tests. The following results can be concluded:

(i) The developed ANN model and regression model can predict the surface Ra ($\mu$m) with high accuracy. The coefficients of determination were found to be about 95% and 94%, for the best neural network model and regression analysis, respectively, from the comparison of the models with thirteen new validation experimental tests that were not used in the modeling phase.

(ii) Maximizing the MRR while keeping the Ra at levels not exceeding a practical value of 0.4 $\mu$m, through multivariable optimization, shows that an optimum MRR of 13680 mm$^3$/min with Ra = 0.283 $\mu$m is obtained at spindle speed 500 rpm, depth of cut 2 mm, and feed rate 200 mm/min.

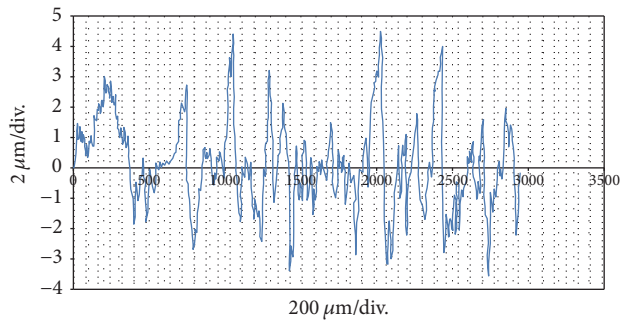


Figure 8: Profile of surface roughness graph by surface roughness tester for machined surface with speed 500 rpm, depth of cut 0.5 mm, and feed rate 150 mm/min.

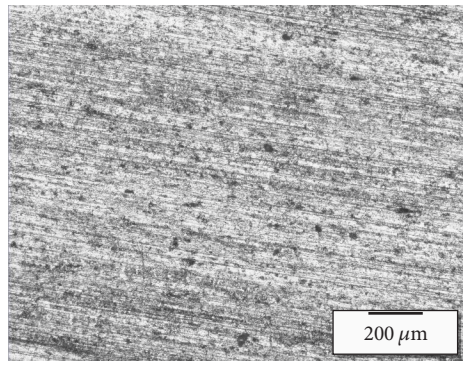


Figure 9: Optical microscopy for machined surface with speed 500 rpm, depth of cut 0.5 mm, and feed rate 50 mm/min.

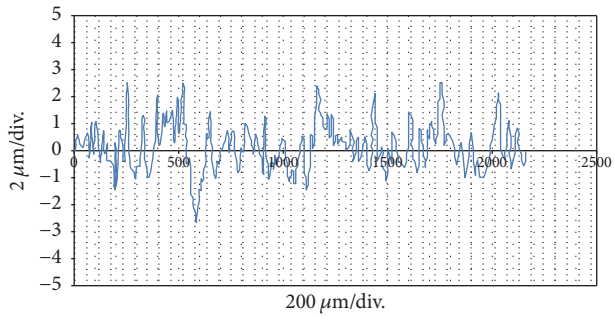


Figure 10: Profile of surface roughness graph by surface roughness tester for machined surface with speed 500 rpm, depth of cut 0.5 mm, and feed rate 50 mm/min.

(iii) Optical microscopy was conducted on two machined surfaces to reveal the effect of feed rate while retaining the value of rpm and depth of cut constant. A hypothetical analysis for relating the higher surface roughness for the higher feed rate is reported.

## Appendix

See Table 4.

Table 4

| Sample ID | Group | Spindle speed (rpm) | Depth of cut (mm) | Table feed (mm/min) | Surface Ra ($\mu$m) | Material removal rate (MRR) $mm^3$/min |
|---|---|---|---|---|---|---|
| 1 | 1 | 500 | 0.5 | 50 | 0.185 | 1000 |
| 2 | | 500 | 0.5 | 100 | 0.226 | 2000 |
| 3 | | 500 | 0.5 | 150 | 0.332 | 3000 |
| 4 | | 500 | 0.5 | 200 | 0.403 | 4000 |
| 5 | 2 | 500 | 1 | 50 | 0.21 | 2000 |
| 6 | | 500 | 1 | 100 | 0.225 | 4000 |
| 7 | | 500 | 1 | 150 | 0.327 | 6000 |
| 8 | | 500 | 1 | 200 | 0.37 | 8000 |
| 9 | 3 | 500 | 1.5 | 50 | 0.177 | 3000 |
| 10 | | 500 | 1.5 | 100 | 0.217 | 6000 |
| 11 | | 500 | 1.5 | 150 | 0.259 | 9000 |
| 12 | | 500 | 1.5 | 200 | 0.313 | 12000 |
| 13 | 4 | 500 | 2 | 50 | 0.164 | 4000 |
| 14 | | 500 | 2 | 100 | 0.174 | 8000 |
| 15 | | 500 | 2 | 150 | 0.22 | 12000 |
| 16 | | 500 | 2 | 200 | 0.248 | 16000 |
| 17 | 5 | 1000 | 0.5 | 50 | 0.133 | 1000 |
| 18 | | 1000 | 0.5 | 100 | 0.184 | 2000 |
| 19 | | 1000 | 0.5 | 150 | 0.197 | 3000 |
| 20 | | 1000 | 0.5 | 200 | 0.245 | 4000 |
| 21 | 6 | 1000 | 1 | 50 | 0.14 | 2000 |
| 22 | | 1000 | 1 | 100 | 0.189 | 4000 |
| 23 | | 1000 | 1 | 150 | 0.207 | 6000 |
| 24 | | 1000 | 1 | 200 | 0.228 | 8000 |
| 25 | 7 | 1000 | 1.5 | 50 | 0.154 | 3000 |
| 26 | | 1000 | 1.5 | 100 | 0.19 | 6000 |
| 27 | | 1000 | 1.5 | 150 | 0.202 | 9000 |
| 28 | | 1000 | 1.5 | 200 | 0.258 | 12000 |
| 29 | 8 | 1000 | 2 | 50 | 0.135 | 4000 |
| 30 | | 1000 | 2 | 100 | 0.2 | 8000 |
| 31 | | 1000 | 2 | 150 | 0.238 | 12000 |
| 32 | | 1000 | 2 | 200 | 0.274 | 16000 |
| 33 | 9 | 1500 | 0.5 | 50 | 0.115 | 1000 |
| 34 | | 1500 | 0.5 | 100 | 0.185 | 2000 |
| 35 | | 1500 | 0.5 | 150 | 0.215 | 3000 |
| 36 | | 1500 | 0.5 | 200 | 0.242 | 4000 |
| 37 | 10 | 1500 | 1 | 50 | 0.156 | 2000 |
| 38 | | 1500 | 1 | 100 | 0.181 | 4000 |
| 39 | | 1500 | 1 | 150 | 0.185 | 6000 |
| 40 | | 1500 | 1 | 200 | 0.224 | 8000 |
| 41 | 11 | 1500 | 1.5 | 50 | 0.137 | 3000 |
| 42 | | 1500 | 1.5 | 100 | 0.149 | 6000 |
| 43 | | 1500 | 1.5 | 150 | 0.217 | 9000 |
| 44 | | 1500 | 1.5 | 200 | 0.24 | 12000 |
| 45 | 12 | 1500 | 2 | 50 | 0.12 | 4000 |
| 46 | | 1500 | 2 | 100 | 0.149 | 8000 |
| 47 | | 1500 | 2 | 150 | 0.191 | 12000 |
| 48 | | 1500 | 2 | 200 | 0.235 | 16000 |
| 49 | 13 | 2000 | 0.5 | 50 | 0.136 | 1000 |
| 50 | | 2000 | 0.5 | 100 | 0.153 | 2000 |
| 51 | | 2000 | 0.5 | 150 | 0.187 | 3000 |
| 52 | | 2000 | 0.5 | 200 | 0.228 | 4000 |

Table 4: Continued.

| Sample ID | Group | Spindle speed (rpm) | Depth of cut (mm) | Table feed (mm/min) | Surface Ra ($\mu$m) | Material removal rate (MRR) $mm^3$/min |
|---|---|---|---|---|---|---|
| 53 | 14 | 2000 | 1 | 50 | 0.153 | 2000 |
| 54 | | 2000 | 1 | 100 | 0.163 | 4000 |
| 55 | | 2000 | 1 | 150 | 0.213 | 6000 |
| 56 | | 2000 | 1 | 200 | 0.22 | 8000 |
| 57 | 15 | 2000 | 1.5 | 50 | 0.14 | 3000 |
| 58 | | 2000 | 1.5 | 100 | 0.155 | 6000 |
| 59 | | 2000 | 1.5 | 150 | 0.217 | 9000 |
| 60 | | 2000 | 1.5 | 200 | 0.228 | 12000 |
| 61 | 16 | 2000 | 2 | 50 | 0.18 | 4000 |
| 62 | | 2000 | 2 | 100 | 0.225 | 8000 |
| 63 | | 2000 | 2 | 150 | 0.255 | 12000 |
| 64 | | 2000 | 2 | 200 | 0.268 | 16000 |

## Conflicts of Interest

The authors declare that they have no conflicts of interest.

## Acknowledgments

This project was supported by King Saud University, Deanship of Scientific Research, College of Engineering Research Center.

## References

[1] A. T. Abbas, A. E. Ragab, E. A. El-Danaf, and E. A. Al Bahkali, "Effect of equal-channel angular pressing on the surface roughness of commercial purity aluminum during turning operation," *Proceedings of the Institution of Mechanical Engineers, Part B: Journal of Engineering Manufacture*, 2016.

[2] E. A. Al Bahkali, A. E. Ragab, E. A. El Danaf, and A. T. Abbas, "An investigation of optimum cutting conditions in turning nodular cast iron using carbide inserts with different nose radius," *Proceedings of the Institution of Mechanical Engineers, Part B: Journal of Engineering Manufacture*, vol. 230, no. 9, pp. 1584–1591, 2016.

[3] A. T. Abbas, A. E. Ragab, E. A. Al Bahkali, and E. A. El Danaf, "Optimizing cutting conditions for minimum surface roughness in face milling of high strength steel using carbide inserts," *Advances in Materials Science and Engineering*, vol. 2016, article 7372132, Article ID 7372132, 14 pages, 2016.

[4] C. Yue, L. Wang, J. Liu, and S. Hao, "Multi-objective optimization of machined surface integrity for hard turning process," *International Journal of Smart Home*, vol. 10, no. 6, pp. 71–76, 2016.

[5] N. Hort, S. N. Mathaudhu, N. R. Neelameggham, and M. Alderman, *Mapping the Mechanical Properties of Alloyed Magnesium (AZ 61), Agilent Technologies*, John Wiley & Sons, Inc., Hoboken, NJ, USA, 2014, article 3788.

[6] S. Chen, B. Shen, and F. Sun, "Experimental optimization of process parameters for turning tc11 titanium alloy using taguchi methodology design," *Key Engineering Materials*, vol. 693, pp. 1009–1014, 2016.

[7] M. Azam, M. Jahanzaib, A. Wasim, and S. Hussain, "Surface roughness modeling using RSM for HSLA steel by coated carbide tools," *International Journal of Advanced Manufacturing Technology*, vol. 78, no. 5, pp. 1031–1041, 2015.

[8] D. Manivel and R. Gandhinathan, "Optimization of surface roughness and tool wear in hard turning of austempered ductile iron (grade 3) using taguchi method," *Measurement*, vol. 93, pp. 108–116, 2016.

[9] K. Raja, P. Marimuthu, and K. Chandrasekaran, "Performance study on aisi316 and aisi410 using different layered coated cutting tools in cnc turning," *Journal of Engineering Science and Technology*, vol. 10, no. 1, 2015.

[10] J. Zhang, S. Y. Liang, and D. Yen, "Optimisation of the finish hard turning process for hardened 52100 steel with PCBN tools," *International Journal of Manufacturing Research*, vol. 2, no. 4, pp. 428–447, 2007.

[11] F. Jafarian, M. Taghipour, and H. Amirabadi, "Application of artificial neural network and optimization algorithms for optimizing surface roughness, tool life and cutting forces in turning operation," *Journal of Mechanical Science and Technology*, vol. 27, no. 5, pp. 1469–1477, 2013.

[12] R. Mokhtari Homami, A. Fadaei Tehrani, H. Mirzadeh, B. Movahedi, and F. Azimifar, "Optimization of turning process using artificial intelligence technology," *International Journal of Advanced Manufacturing Technology*, vol. 70, no. 5–8, pp. 1205–1217, 2014.

[13] F. Jafarian, D. Umbrello, S. Golpayegani, and Z. Darake, "Experimental Investigation to Optimize Tool Life and Surface Roughness in Inconel 718 Machining," *Materials and Manufacturing Processes*, vol. 31, no. 13, pp. 1683–1691, 2016.

[14] N. M. Vaxevanidis, N. A. Fountas, J. D. Kechagias, and D. E. Manolakos, "Optimization of main cutting force and surface roughness in turning of TI-6AL-4V titanium alloy using design of experiments and artificial neural networks," in *Proceedings of 1st International Conference on Engineering and Applied Sciences Optimization, OPT-i 2014*, pp. 2889–2906, 2014.

[15] S. Senthil Babu and B. K. Vinayagam, "Surface roughness prediction model using adaptive particle swarm optimization (APSO) algorithm," *Journal of Intelligent and Fuzzy Systems*, vol. 28, no. 1, pp. 345–360, 2015.

[16] G. Orcen, S. Bingol, and M. Gur, "Modelling and comparison of failure load with FEM and ANNs. of Composite Materials," *Journal of Composite Materials*, pp. 10–1177, 2015.